First steps with HLLMHD and PP reconstruction: Part IV

by *O. Steiner*

Part IV revisits part I of the present report. We repeat calculations with the same solar model, varying a number of parameters and using the CO5BOLD-code version for_2012.11.05b instead of version for_2011.04.28 that was used in parts I-III. We are now also experimenting with the newly available FRweno reconstruction, a scheme that was designed by Bernd Freytag to be less diffusive than the van Leer linear reconstruction but less aggressive than PP. In addition, we have carried out test calculations with models of higher spatial resolution. The size of the boxes is always 4.8 Mm $\times$ 4.8 Mm $\times$ 2.8 Mm. The $\tau = 1$ level is at a height of about 1.5 Mm from the bottom. The grid cells of the low resolution boxes have a horizontal width of 40 km and a vertical extent varying from 50 km in the bottom part of the convection zone to 20 km in the top part of the convection zone, the photosphere, and the chromosphere. The initial model consists of relaxed convection as computed with HLLMHD and Van Leer reconstruction. The initial magnetic field is homogeneous and vertical with a strength of 50 G. For certain runs with FRweno, we have done a regridding for equidistance in z-direction. In this case, the vertical size of the cells is 20 km constant. The high resolution grids have either 20 km or 10 km equidistant cell sizes in all directions. For the 10 km resolution runs, the parameter `N_radsubray` was set to 1 while it is 2 for all other runs and the parameter `N_radtaurefine` was set to 2, while it is 3 in all other runs. The parameter `N\radthickpoint` is set 80 in the 10 km resolution run, 30 in the 20 km resolution run, and 0 in all other runs. For all models $\nu_{\rm art} = 0.0$ but $\nu_{\rm Smagorinsky}$ is either 0.5 or 0.0. and all models were run for 540 s. Table 1 shows a compilation of the models and runs for this part of the report.

job/run	solver	integration	reconstr.	$\nu_{\rm Smag.}$	$B_{\rm init}$	initial model	$t_{\rm end}$
job_vanleer_hancock_b							
rhd_vl_hck_b	HLLMHD	Hancock	VanLeer	0.5	$B_z = 50$ G	rmhd120x120x120_v50	540 s
job_pp_hancock_b/test							
rhd_pp_hck	HLLMHD	Hancock	PP	0.5	$B_z = 50$ G	rmhd120x120x120_v50	540 s
rhd_pp_hck_a	HLLMHD	Hancock	PP	0.0	$B_z = 50$ G	rmhd120x120x120a_v50	540 s
rhd_radcourant	HLLMHD	Hancock	PP	0.5	$B_z = 50$ G	rmhd120x120x120_v50	540 s
rhd_visp2pincl1	HLLMHD	Hancock	PP	0.5	$B_z = 50$ G	rmhd120x120x120_v50	540 s
rhd_vissmagorinsky	HLLMHD	Hancock	PP	0.0	$B_z = 50$ G	rmhd120x120x120_v50	540 s
rhd_einteq	HLLMHD	Hancock	PP	0.0	$B_z = 50$ G	rmhd120x120x120_v50	540 s
rhd_RK3	HLLMHD	RungeKutta3	PP	0.0	$B_z = 50$ G	rmhd120x120x120_v50	540 s
rhd_unsplitRK3	HLLMHD	RungeKutta3	PP	0.0	$B_z = 50$ G	rmhd120x120x120_v50	540 s
rhd_PPa_480x480	HLLMHD	Hancock	PP	0.0	$B_z = 50$ G	rmhd480x480x280_v50	540 s
job_FRweno_hancock_b							
rhd_FRweno	HLLMHD	Hancock	FRweno	0.5	$B_z = 50$ G	rmhd120x120x120_v50	540 s
rhd_FRweno_vissmag0	HLLMHD	Hancock	FRweno	0.0	$B_z = 50$ G	rmhd120x120x120_v50	540 s
rhd_FRwenoa_vissmag0	HLLMHD	Hancock	FRweno	0.0	$B_z = 50$ G	rmhd120x120x120_v50	540 s
rhd_FRwenoa	HLLMHD	Hancock	FRweno	0.5	$B_z = 50$ G	rmhd120x120x120_v50	540 s
rhd_FRwenoa_240x240	HLLMHD	Hancock	FRweno	0.5	$B_z = 50$ G	rmhd240x240x140_v50	540 s
rhd_FRwenoa_480x480	HLLMHD	Hancock	FRweno	0.5	$B_z = 50$ G	rmhd480x480x280_v50	540 s

Table 1: Various models and runs for part IV. For rhd_radcourant, c_radcourant was set from 2.4 to 0.4 and c_radcourantmax from 2.6 to 0.6. For rhd_visp2pincl1 c_visp2pincl1 was set 0.0 instead of 1.0. For rhd_einteq, beta_inv was set 0.0 instead of 10.0. For rhd_RK3, the time integration was done with RungeKutta3. For rhd_unsplitRK3, hdsplit = unsplit and hdtimeintegrationscheme = RungeKutta3.

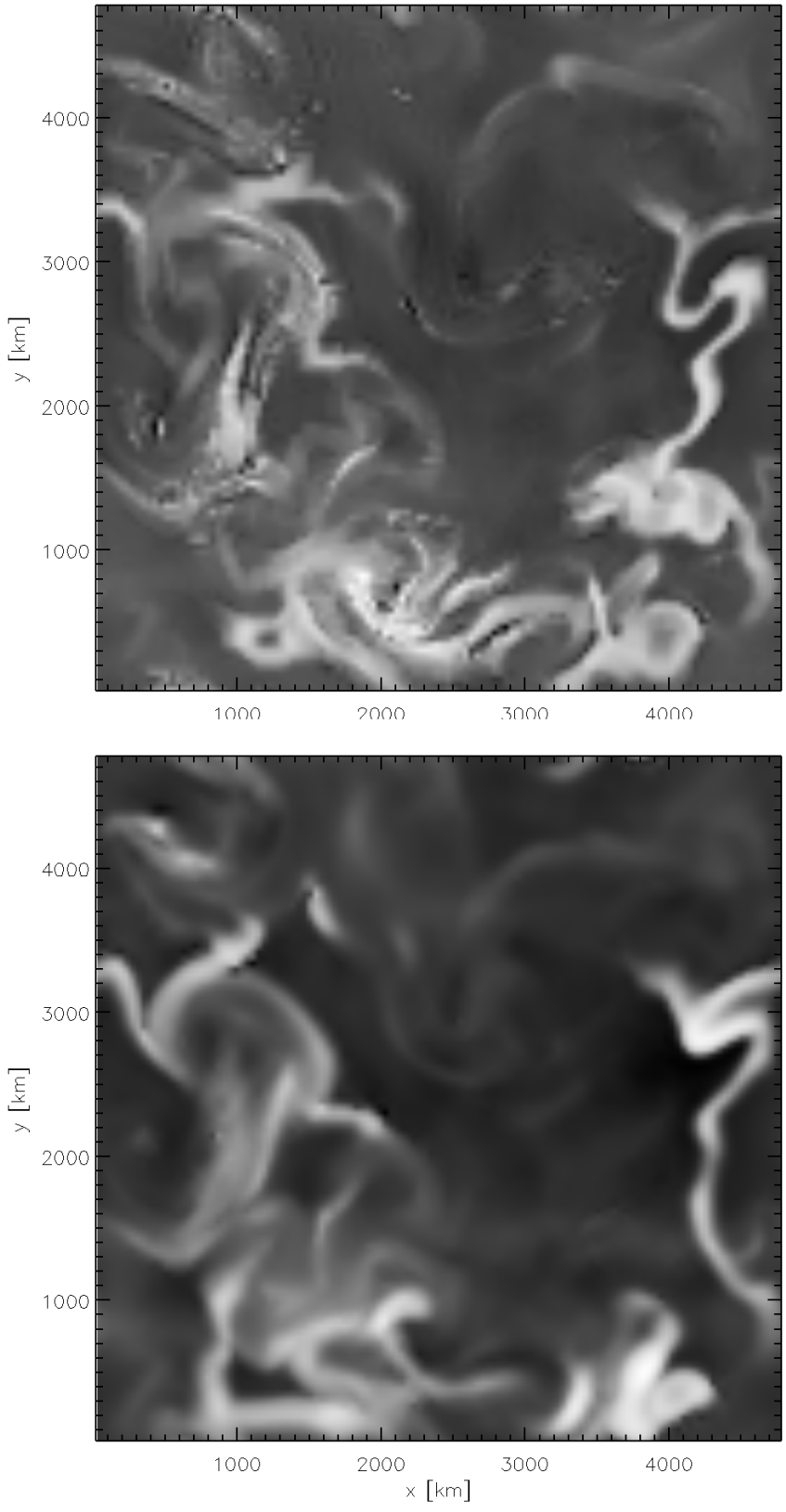

Figure 1: Temperature at a level of 1200 km above $\langle\tau\rangle = 1$ after 540 s, starting from a solar model with an initial vertical homogeneous magnetic field of 50 G. Low resolution with $120 \times 120 \times 120$ grid points. Top panel: Simulation with PP reconstruction. Bottom panel: Simulation with FRweno reconstruction.

Temperature

A major problem that became apparent in part I of this report was that the horizontal sections in the temperature at chromospheric heights of magnetic models showed strong wiggles, sawteeth, and single cool pixels when using the PP reconstruction. This problem was completely absent for magnetic field-free models and also for magnetic models when using the van Leer reconstruction (see Figs. 10 and 4 of part I, respectively). It was therefore of great interest to find out whether this problem persists with the new code version and wether FRweno was doing a better job than PP.

Figure 1 shows the temperature at a level of 1200 km above $\langle\tau\rangle = 1$ after 540 s starting with an initially vertical, homogeneous magnetic field of 50 G. This is a low resolution simulation with $120 \times 120 \times 120$ grid points. As expected, FRweno (run rhd_FRweno) is more diffusive than PP (run rhd_pp_hck) but the solution shows much more details than the VanLeer solution (see Fig. 4 (top) of part I) and most details of the PP solution. The *good news* are that FRweno shows much less saw teeth and cool pixels than PP. The solution with FRweno was in this case obtained with a grid that is non-equidistant in the z-direction. This means that PP is still in use in that direction. When using a fully equidistant grid the solution becomes smoother, once more, with fewer cool pixels. Finally, when setting c_vissmagorinsky = 0 (run rhd_FRwenoa_vissmag0), the cool pixels virtually disappear. This solution is shown in Fig. 2, once more together with the solution obtained with PP on the same equidistant grid (run rhd_pp_hck_a), for comparison.

Also from Figs. 1 and 2, we can see that the problems with the PP reconstruction at chromospheric heights remain with the new code version.

Experiments with the PP reconstruction scheme

Once again, I attempted to improve the solution obtained with PP by varying a number of parameters—without success. In what follows is an account of these trials. The parameter file of the new code differs from the old code version because of various additional features. I started with a parameter file that I judged most similar to the old one and obtained a solution for the temperature in the horizontal section at $z = 1200$ km (see Fig.1) (top) that is quite similar to the old one shown in Fig. 4 (bottom) of part I of this report. The new PP solution looks slightly more diffusive and has more cool pixels, but not cooler pixels. In the old run, the temperature varied between 2120 K and 5747 K, in the present run it varies between 2663 K and 5942 K.

A change of c_radcourant from 2.4 to 0.4 and c_radcourantmax from 2.6 to 0.6 (run rhd_radcourant) had no appreciable effect despite the fact that the time step was reduced from typically 0.3 s to 0.1 s. Going back to c_radcourant = 2.4 and c_radcourantmax = 2.6 and changing c_visp2pincl1 from 1.0 to 0.0 had no appreciable effect (run rhd_visp2pincl1). In fact, the temperature range at time 540 s stays exactly the same indicating that the parameter c_visp2pincl1 is not rekcognized by the MHD module at all.

Next we set c_visp2pincl1 back to 1.0 and set c_courant from 0.8 back to the old value 0.5 and c_courantmax from 0.9 back to the old value 0.7. From the experience

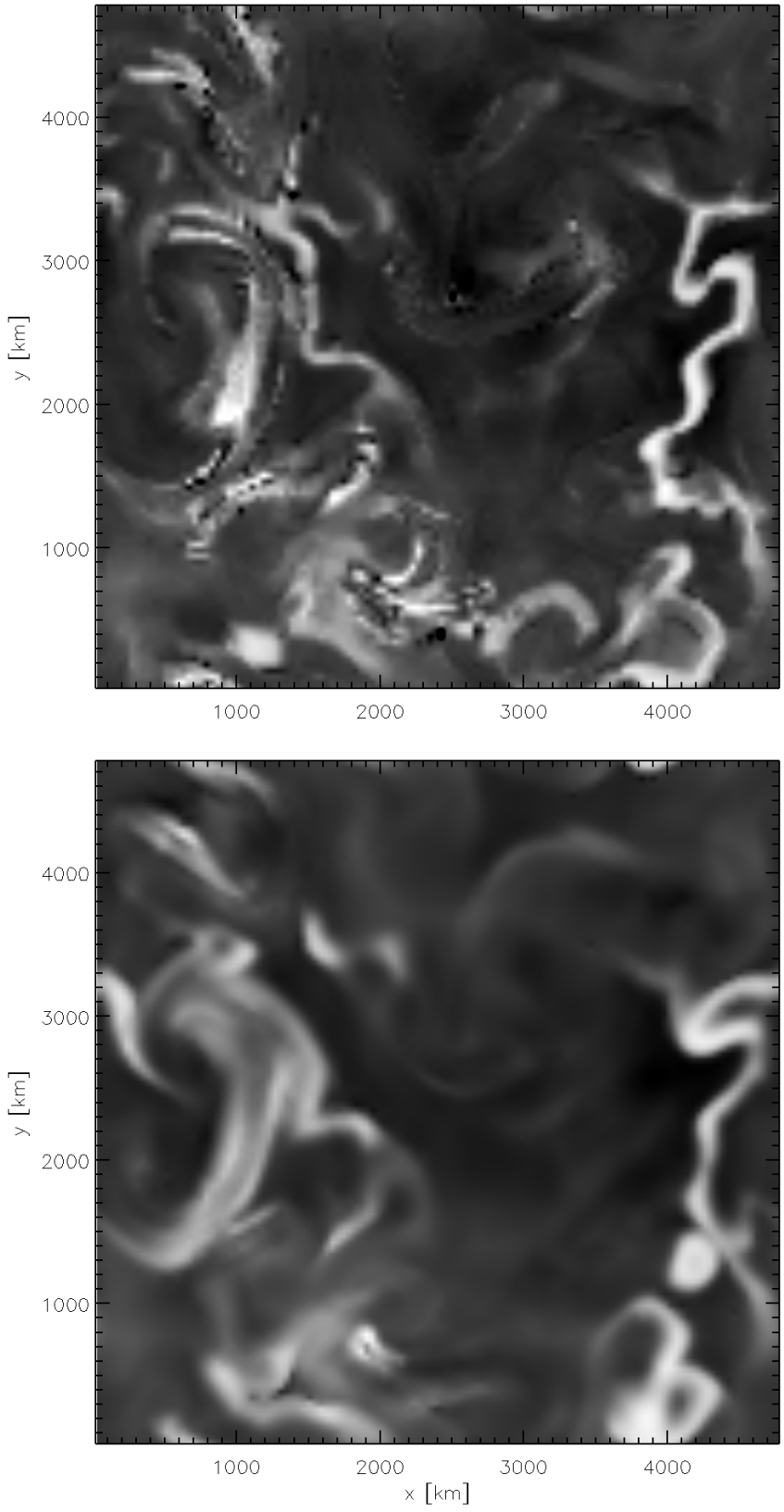

Figure 2: Temperature at a level of 1200 km above $\langle\tau\rangle = 1$ after 540 s. Fully equidistant grid, Hancock time integration, and c_vissmagornsky = 0. Top: Run rhd_pp_hck_a with PP reconstruction. Bottom: Run rhd_FRwenoa_vissmag0 with FRweno reconstruction.

with c_radcourant we can't expect any major changes, which indeed is the case. The temperature in the section at $z = 1200$ km varies between 2340 K to 5938 K. There is no striking difference with respect to the original solution shown on the bottom panel of Fig. 4, part I of this report.

Leaving c_courant and c_courantmax at 0.5 and 0.7, respectively, and setting n_orderconstrainedtransport = 1 instead of until now 2 has virtually no effect as was already experienced in part I of this report.

Next we set c_courant and c_courantmax back to 0.8 and 0.9, respectively, and n_orderconstrainedtransport back to 2 and we set c_visbound = 0.0 instead of 0.5 as it was so far. In this case, there are differences visible but no major ones in the temperature section at $z = 1200$ km. The temperature is generally a bit higher in large, cool areas (pressumably less adiabatic dilution in downflow regions near the top) but the single cool pixels remain as before.

Setting back c_visbound = 0.5 and set c_vissmagorinsky = 0.0 results in a slightly less diffusive solution but the cool pixels remain (run rhd_vissmagorinsky).

When setting beta_inv = -1.0 so that only the total energy equation is used, time steps become very small, in the order of milliseconds, and along shock fronts, pixels with temperatures as low as 1300 K appear already after 0.1 s. This job was aborted after 6 s.

When setting beta_inv = 0.0 so that the internal energy equation is used throughout (run rhd_einteq), the solution ($T(z = 1200$ km$)$, see Fig. 3, top) looks definitely better than that of all previous runs with PP. There are still cool pixels along temperature fronts but the variation of the temperature over the whole domain is smaller (2720 K to 5725 K) compared to rhd_pp_hck, where it varied between 2666 K and 5943 K.

Next set back betainv = 10.0 and set hdtimeintegrationscheme = RungeKutta3 (run rhd_RK3). This results in a solution (T(z=1200 km)), which is distinctly different from the one under job_pp_hancock_b but the cool pixel problem remains. The temperature varies between 2241 and 6176 K.

Going back to the Hancock time integration but setting hdsplit = unsplit leads immedediately to a crash in the first time step (segmentation fault). Reduction of the time step by either, setting dtime_start = 1.0E-03 or reducing dtime_max to 1.0E-03 does not help. When setting, additionally to hdsplit = unsplit, hdtimeintegrationscheme = RungeKutta3 (run rhd_unsplitRK3), the program works fine and does not crash. The solution after 540 s looks best resolved of all previous runs but the cool pixel problem remains. The temperature varies at $z = 1200$ km from 2550 K to 5816 K. The solution looks again more similar to the previous solutions (under job_pp_hancock_b) and different from rhd_RK3.

Later, I realized that increasing KMP_STACKSIZE to 128m (from former 16m) solves the problem with unsplit plus Hancock and the job does not immediately crash anymore. However, when setting c_vissmagorinsky = 0, it crashes after about 440 s because of a too small time step but it runs without crashing when c_vissmagorinsky = 0.5. The corresponding solution is shown in Fig. 3, bottom. The cool pixel problem remains.

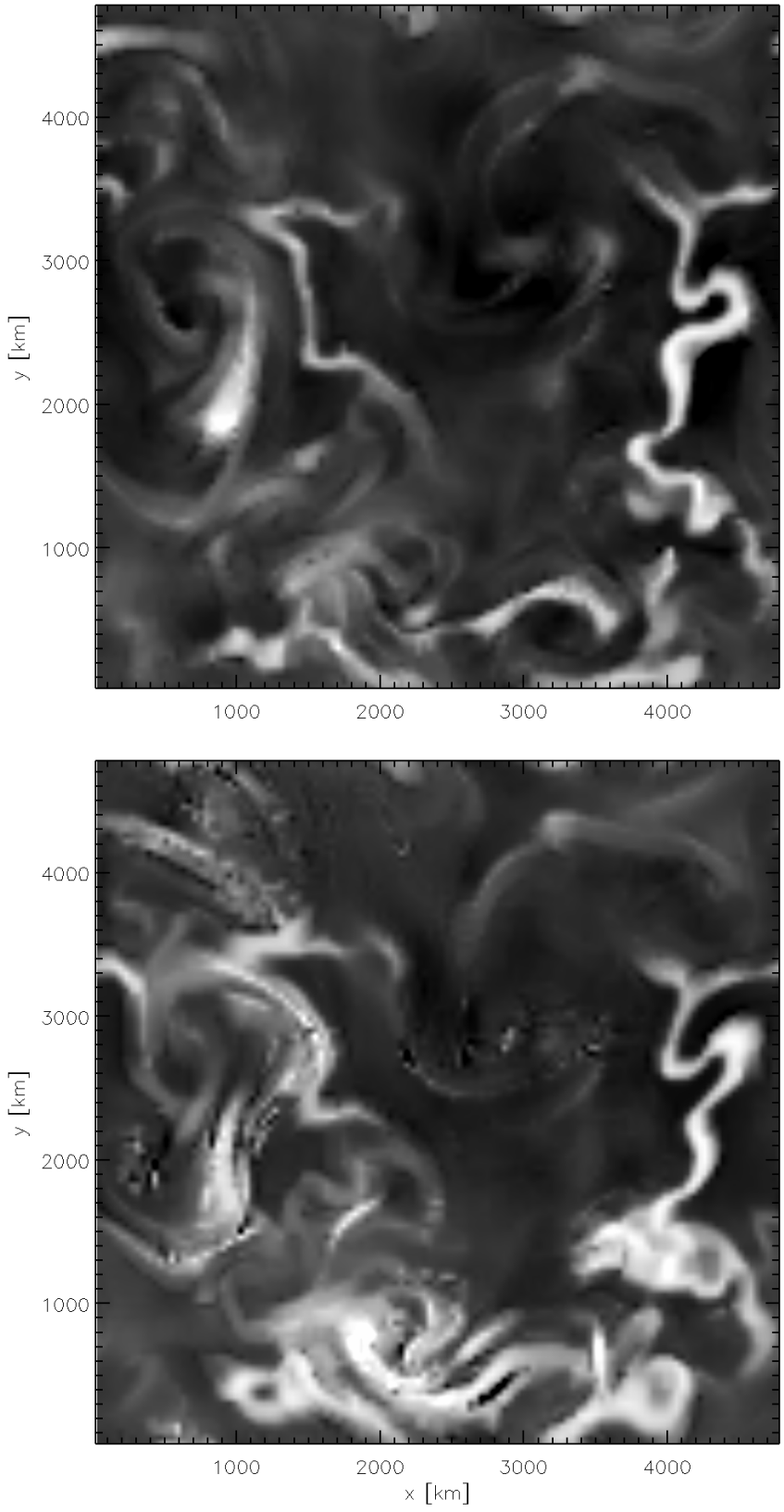

Figure 3: Temperature at a level of 1200 km above $\langle\tau\rangle = 1$ after 540 s. Hancock time integration and PP reconstruction. Top: beta_inv = 0.0 so that the internal energy equation is used only, c_vissmagorinsky = 0, and hdtimeintegration = 123. Bottom: beta_inv = 10.0, c_vissmagorinsky = 0.5, and hdtimeintegration = unsplit.

Experiments with the FRweno reconstruction scheme

Figure 1 (bottom) shows the solution computed with hdtimeintegrationscheme = Hancock, reconstruction = FRweno, hdsplit = 123, and c_vissmagorinsky = 0, corresponding to run rhd_FRweno_vissmag0. It looks fine with a few minor cool pixels close to the top boundary. Around $\tau = 1$, $T(x,y)$ looks smoother and less pixelated than PP. In the convection zone, the temperature with FRweno looks slightly more "compact" and less diffusive than with PP. This, however, cannot be said of the velocity components, which in turn look definitely more diffusive in the convection zone with FRweno. In the chromosphere, the temperature looks much nicer but definitely more diffusive than with PP. This can also be said of the velocities.

When setting c_vissmagorinsky back to 0.5 (rhd_FRweno), the solution is only slightly more diffusive, but we get back to the problem with cool pixels in the chromosphere. Not as bad as with PP, but definitely worse than with c_vissmagorinsky=0. In particular at $(ix, iy, iz) = (8, 73, 114)$ we get a pixel with $T = 2036$ K, while the corresponding run with c_vissmagorinsky = 0 has at this same location $T = 3708$ K without any conspicuity.

Next, we generated a start file with equidistant grid points in the z-direction (rmhd120x120x120_v50a.sta instead of old rmhd120x120x120_v50.sta). This new start file has 140 cells in the z-direction (instead of 120 up to now) with $\Delta_z = 20$ km. In this case, FRweno is used in all three spatial directions while up to now FRweno was used in the equidistant x and y-direction only while PP was in use in the non-equidistant z-direction. When setting c_vissmagorinsky = 0.5 (run rhd_FRwenoa), the solution looks very similar to the solution with the non-equidistant z-grid points but the cool pixel problem is less severe and the problem at $(ix, iy, iz) = (8, 73, 114)$ disappears. When setting c_vissmagorinsky = 0.0 (run rhd_FRwenoa_vissmag0), the solution with equidistant grids (see Fig. 2) is very similar to the one with the non-equidistant grid but the cool pixel problem in the chromosphere becomes once again relaxed and is virtually absent. Thus, FRweno basically resolves the problem with cool pixels and sawteeths while keeping almost as much details as PP.

Figure 4 shows another comparison in temperature between PP and FRweno. Both panels show the temperature in the horizontal section at a height of 60 km above the level of optical depth $\tau = 1$. In these sections, one can see the “hot walls” of magnetic flux concentrations. The top panel refers to the run rhd_pp_hck_a computed on the equidistant grid with PP, the bottom panel to run rhd_FRwenoa_vissmag0 on the same equidistant grid with FRweno. Both runs went with c_vissmagorinsky = 0. Again, FRweno is slightly more diffusive than PP but does a much better job with the hot walls. This is important in view of studies regarding brightness contributions of magnetic elements in the solar and stellar atmospheres and corresponding energetic considerations.

Figure 5 shows the emergent bolometric intensity of the same two models and snapshots as of Figure 4. As can be expected from Figure 4, the enhanced intensities at locations of magnetic flux concentrations is smoother when computed with FRweno than in case of PP. On the other hand, the granulation is clearly more diffusive in case of FRweno compared to PP.

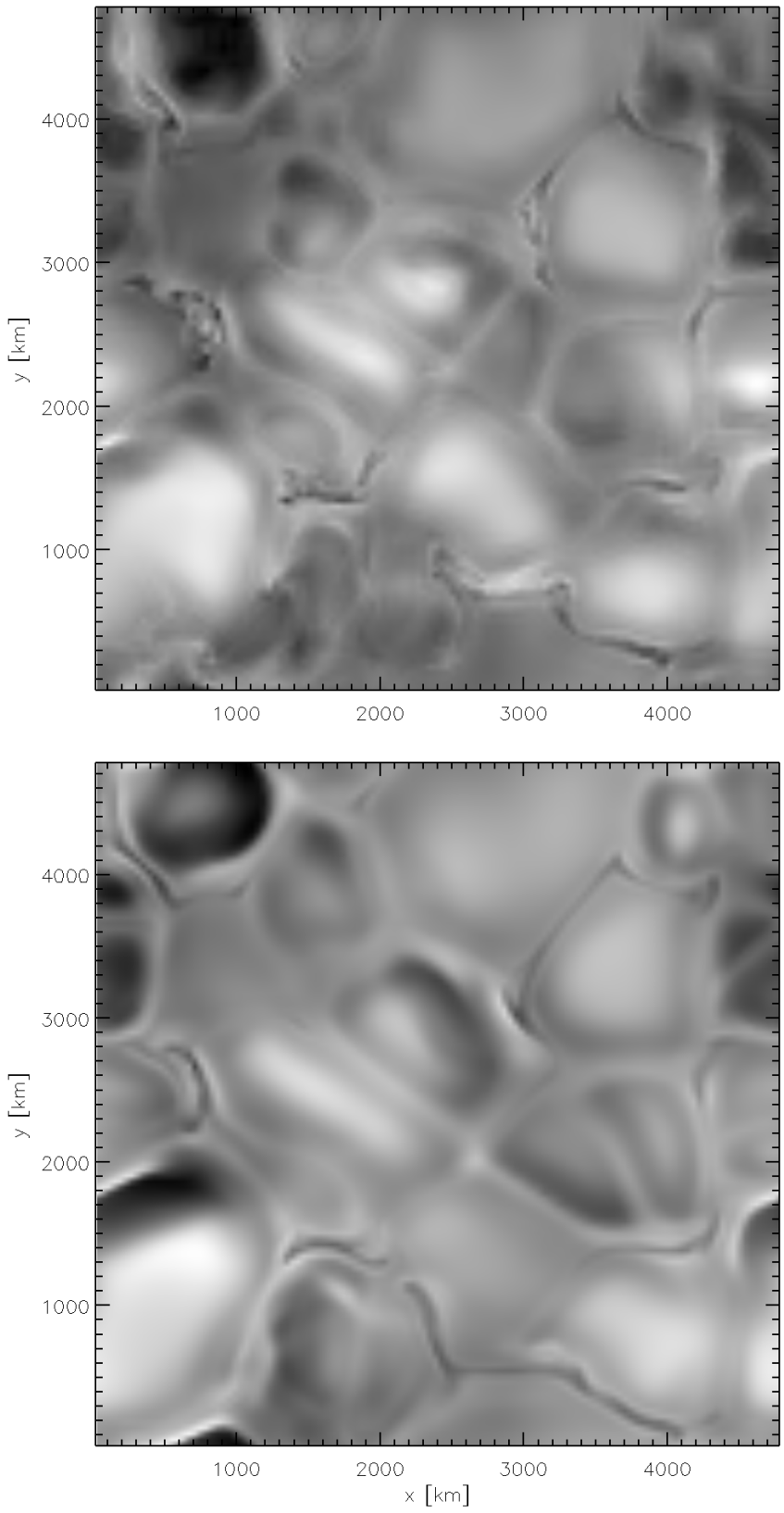

Figure 4: Temperature at a level of 60 km above $\langle\tau\rangle = 1$ after 540 s. Fully equidistant grid and c_vissmagorinsky = 0. Top: PP, Botto: FRweno.

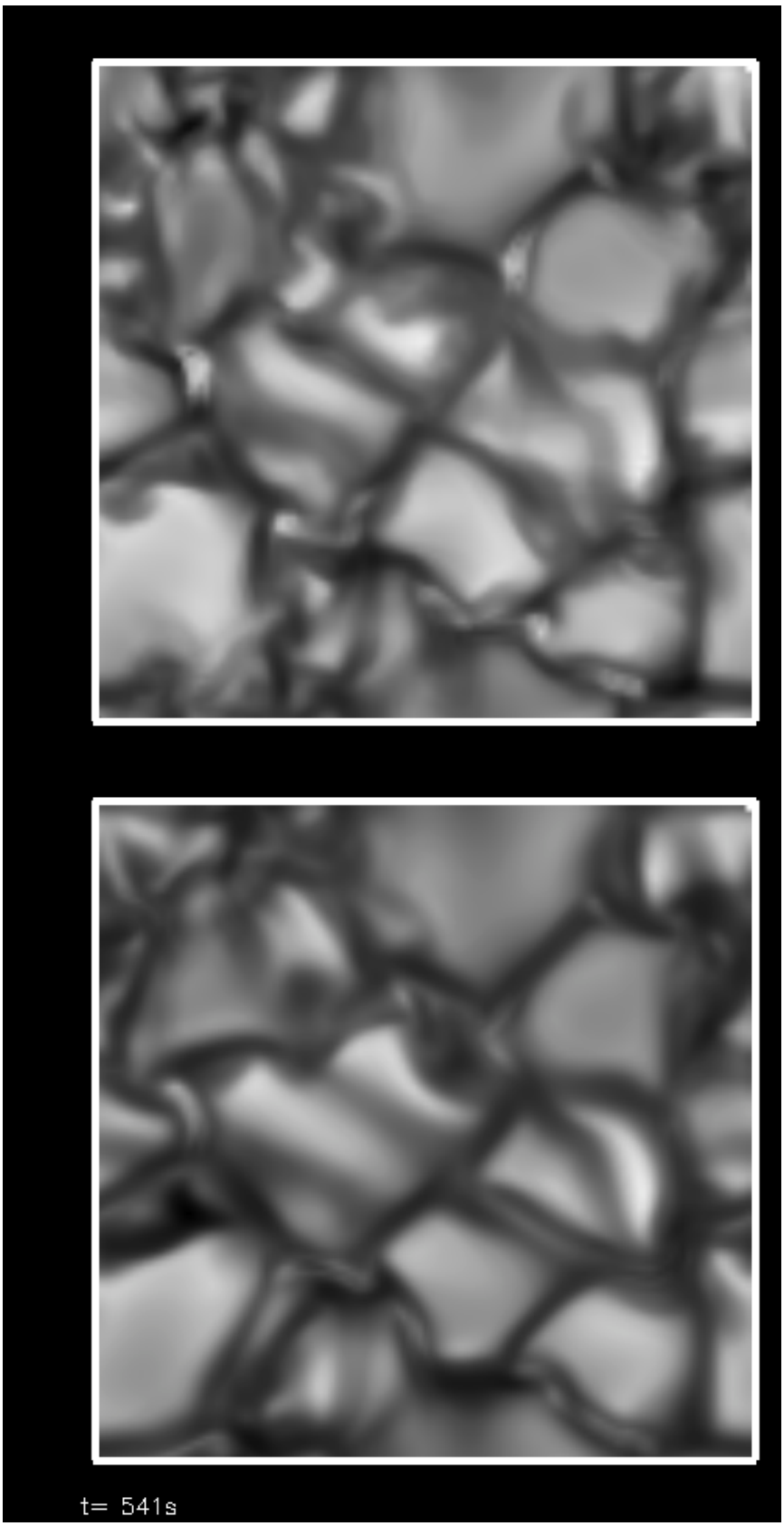

Figure 5: Emergent bolometric intensity after 540 s. Fully equidistant grid and c_vissmagorinsky = 0. Top: PP, Botto: FRweno.

Runs with higher spatial resolution

Figure 5 suggests that these simulations are way under-resolved, in particular with regard to the "filigree" which consists of the bright filaments in the intergranular space at locations of magnetic flux concentrations. I have therefore carried out equivalent test runs with a grid of $240 \times 240 \times 140$ cells with equidistant cell sizes of 20 km in all spatial directions and with a grid of $480 \times 480 \times 280$ cells with equidistant cell sizes of 10 km in all spatial directions. Note that the following figures are best viewed on the screen.

The result are shown in Fig. 6, which indeed confirms that the solutions have not yet converged: the filigree becomes thinner and more delicate with increasing resolution. Also the magnetic field shows more substructure with increasing resolution: especially noteworthy is the folding at $(x,y) \sim (3100,3300)$ km or the swirl at $(x,y) \sim (800,2700)$ km. Also, the 10 km resolution run shows ample opposit polarity magnetic fields along magnetic filaments, which is virtually absent in the lowest resolution run. It looks like a resolution of 10 km is absolutely necessary for a 'realistic' simulation of the filigree.

I have also carried out a high-resolution run with PP. The result is shown in Fig. 7. PP shows even more details of the filigree than FRweno and even more so of the granules. The temperature in a horizontal section at $z = 60$ km however shows strong 'pixellation' in the case of PP. This, however, seems not to have a negative influence of the emergent intensity as the latter is an integral quantity. Also the vertical magnetic field component at $z = 0$ looks fine. This suggests that PP may still be a good choice for certain applications.

Coming back to the top (chromospheric) layers, one can first say that the temperature structure with PP in these layers improves with increasing resolution but the problem with saw teeth and cool pixels remains. This is shown in Fig. 8, which shows the temperature in a horizontal section 1200 km above $\langle\tau\rangle = 1$ as computed on the 10 km resolution grid, once with PP (top) and once with FRweno (bottom). The temperature varies in this section between 2100 K and 6800 K with PP and between 2400 K and 6200 K with FRweno. The two solutions differ substantially after 540 s simulation time.

Figure 9 shows the temperature and the horizontal velocity at $z = 1200$ km and at three different spatial resolutions. We see from this figure that the solutions at chromospheric heights differ substantially between the different resolutions and that convergence has by far not been reached. We clearly see the swirls that are generated by action of the magnetic field (solar tornadoes) but these seem to become less coherent at higher spatial resolution.

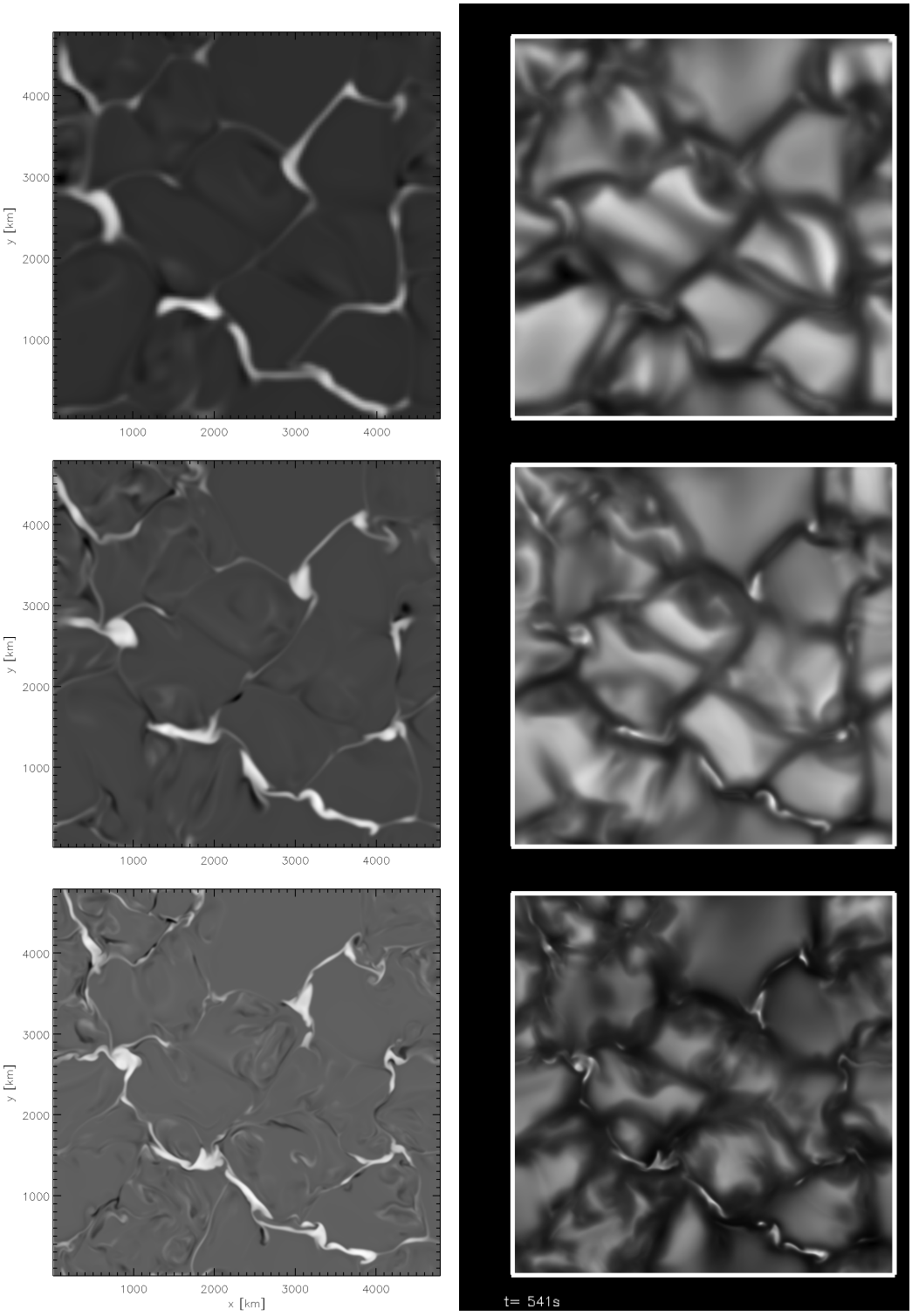

Figure 6: Runs of varying spatial resolutions using FRweno reconstruction and Hancock time integration. The parameter c_vissmagorinsky was set to 0. Left column: Vertical magnetic field strength at the height $z = 0$. Right column: Emergent bolometric intensity. Fully equidistant grids with, Top row: $120 \times 120 \times 140$ grid cells, Middle row: $240 \times 240 \times 140$ grid cells, and, Bottom row: $480 \times 480 \times 280$ grid cells.

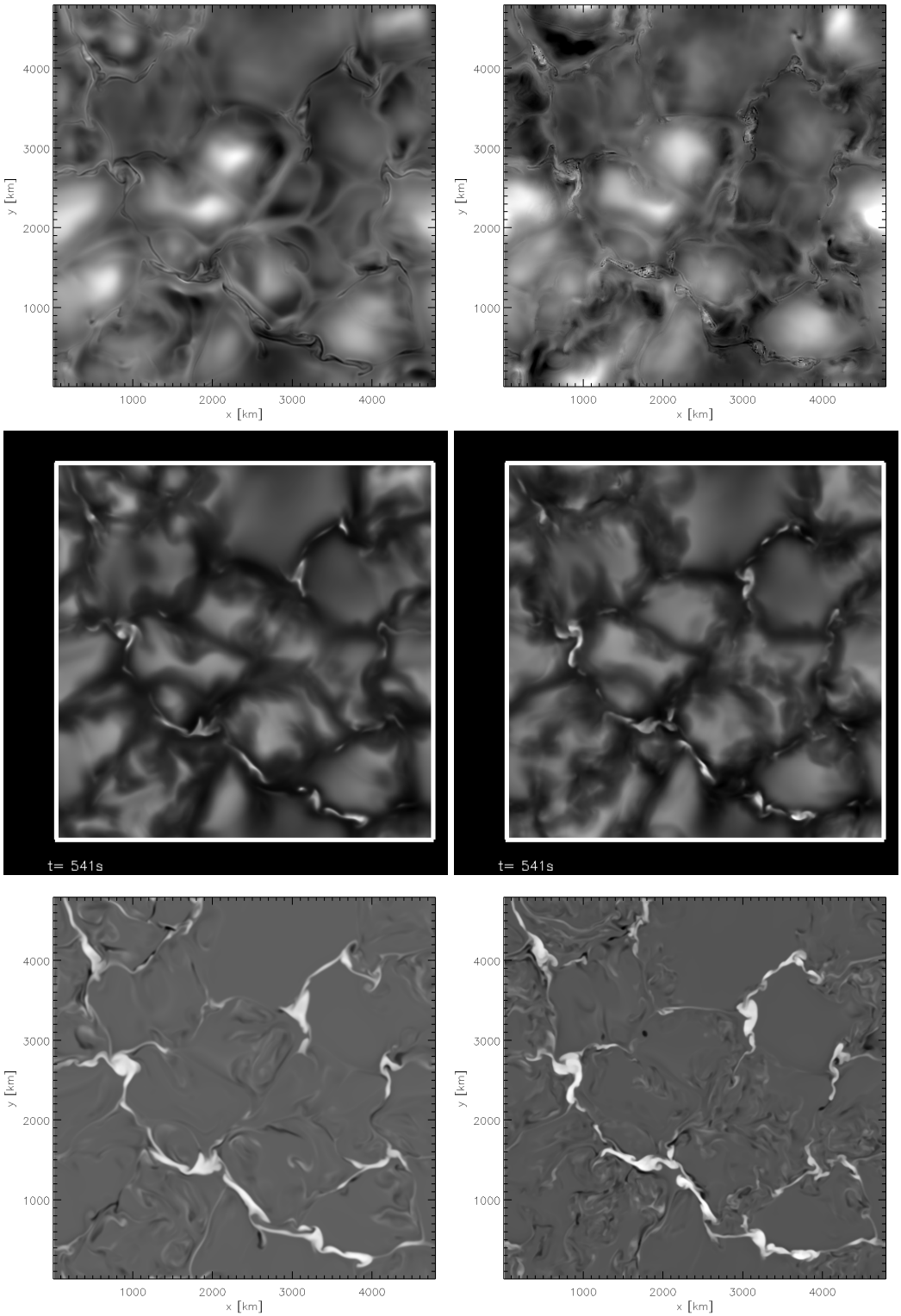

Figure 7: High-resolution run on an equidistant grid with 10 km cell widths and $480 \times 480 \times 280$ cells. Hancock time integration, c_vissmagorinsky = 0. Left column: FRweno reconstruction. Right column: PP reconstruction. From top to bottom: $T(z = 60$ km, Bolometric intensity, $B_z(z = 0)$. Left column: Vertical magnetic field strength at the height $z = 0$.

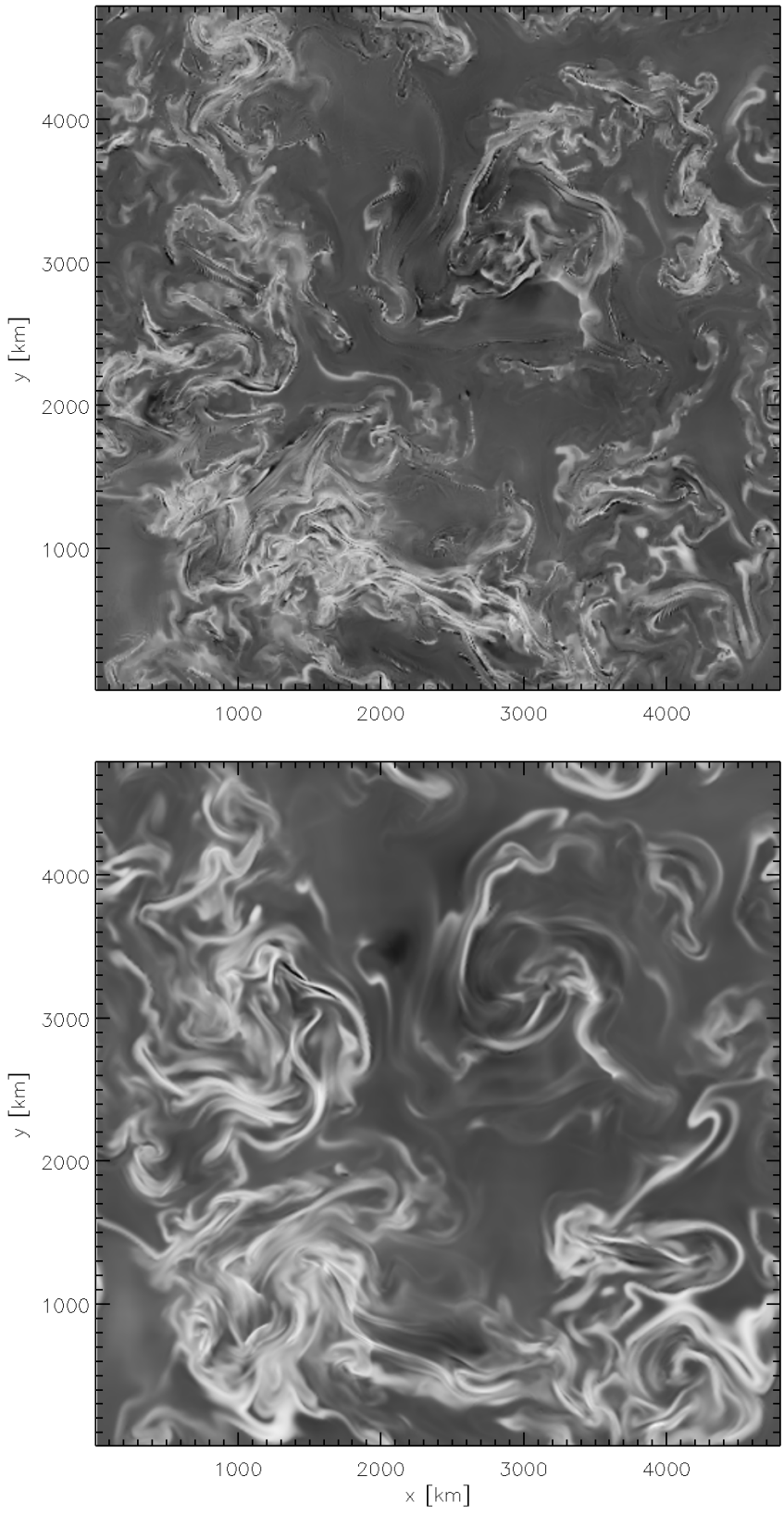

Figure 8: $T(z = 1200\ \text{km})$ on the 10 km resolution grid. Top: PP, Bottom: FRweno.

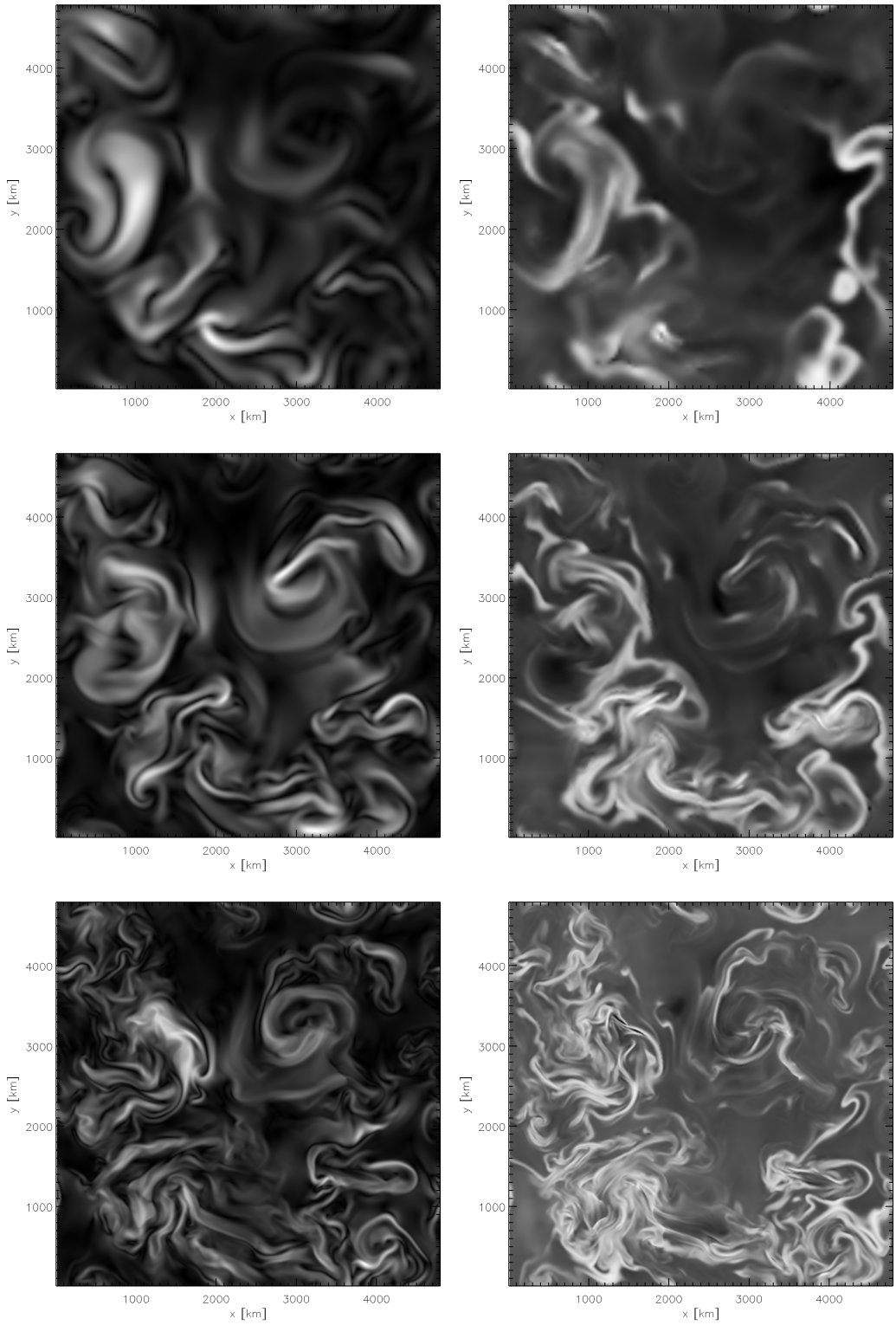

Figure 9: High-resolution run on an equidistant grid with 10 km cell widths and $480 \times 480 \times 280$ cells. Hancock time integration, FRweno reconstruction scheme and c_vissmagorinsky = 0. Left column: Absolute horizontal velocity at $z = 1200$ km. Right column: Temperature at $z = 1200$ km.

A bug concerning VanLeer in combination with directional splitting?

Strangely, the new version for_2012.11.05b produces a solution quite dissimilar from the old one produced with for_2011.04.28, when running with Van Leer reconstruction and Hancock time integration. The deviation is large only close to the top boundary, encompassing about the top 300 km. There, the temperature fluctuations are much larger with for_2012.11.05b. The velocities do not show any conspicuous differences The difference can readily be seen from Fig 10, which shows the temperature 1200 km above $\langle\tau\rangle = 1$. The temperature in this horizontal section fluctuates between 3110 K and 5480 K in the old solution, while the new one shows a corresponding fluctuations between 1650 K and 5730 K.

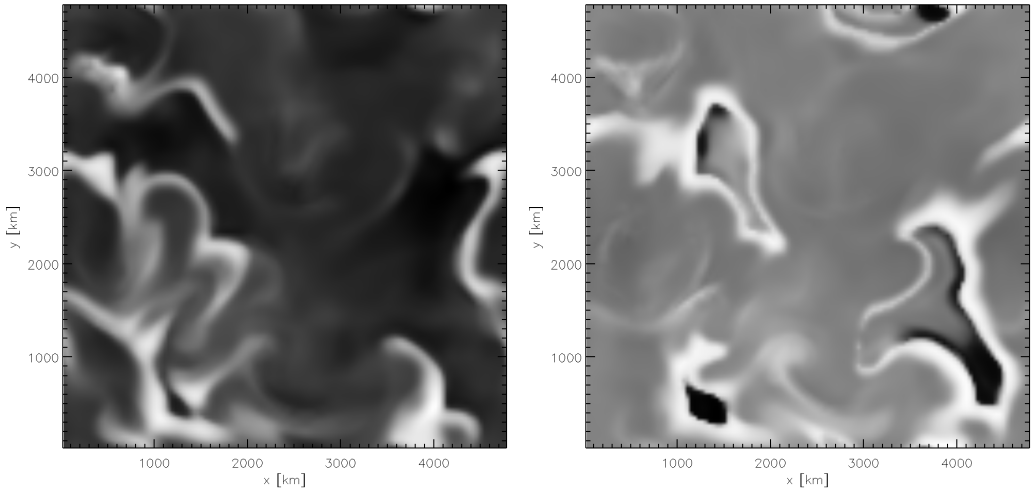

Figure 10: Temperature in the horizontal section at 1200 km above $\langle\tau\rangle = 1$. Left: Computation with the old code version, for_2011.04.28. Right: Computation with the new code version, for_2012.11.05b. Both runs with VanLeer reconstruction, Hancock time integration, and directional splitting.

In order to find the origin of this discrepancy, I have adjusted parameters towards the old values that were in use with for_2011.04.28. First, I lowered the value of parameter c_tchange from 0.3 to 0.1 (run rhd_vl_hck_tchange0p1), then, I set additionally c_radhtautop = 100.0E+05 instead of -1.0 (run rhd_vl_hck_radhtautop), and finally I set additionally c_courant = 0.5 and c_courantmax = 0.7 instead of previously 0.8 and 0.9, respectively, and c_radcourant = 0.5 and c_radcourantmax = 1.5 instead of previously 2.4 and 2.6, respectively (run rhd_vl_hck_courant). All these changes did not lead to success and the problem persisted. In fact, differences between these runs were hard to notice.

When running PP reconstruction and Hancock time integration, the differences between the old run with for_2011.04.28 and the new ones with for_2012.11.05b are much smaller, also close to the top boundary. It looks as if there was a bug in the top boundary conditions that concerns only VanLeer.

Furthermore, I varied the followingg parameters. Setting c_tminlimit = -1.0 in-

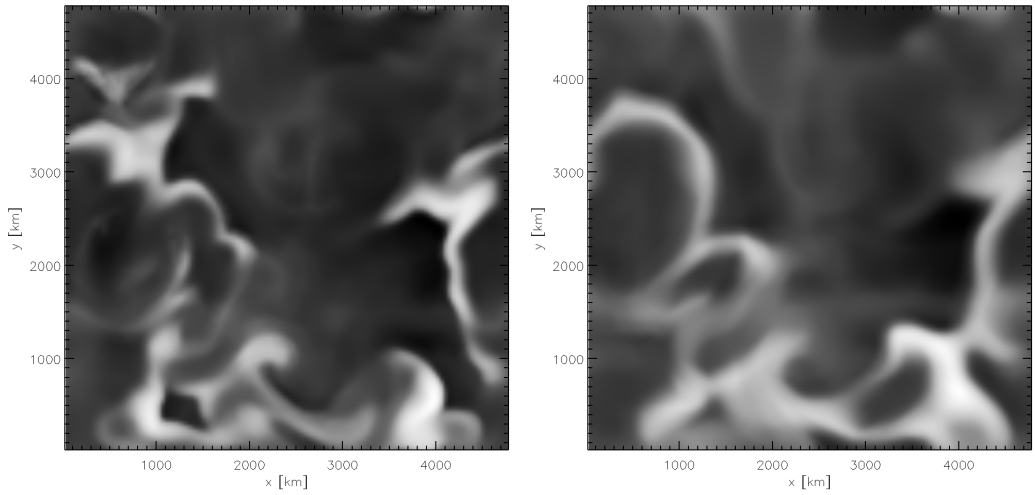

Figure 11: Temperature in the horizontal section at 1200 km above $\langle\tau\rangle = 1$. Left: VanLeer and hdsplit = unsplit. Right: Minmod and hdsplit = 123.

stead of 1600.0 and setting c_visbound = 0.0 instead of 0.5 (run rhd_vsiboun_tlimit) did not result in large differences. Using hdtimeintegrationscheme = RungeKutta3 (run rhd_RK3) does not help neither. Also changing c_rhochangetop from 0.0 to 0.2 did not help (run rhd_rhochangetop).

Interestingly, when setting hdsplit = unsplit (together with the Hancock time integration and the van Leer reconstruction scheme, run rhd_unsplit_hck), we get back to normal temperature fluctuations at $z = 1200$ km, namely between 3086 K and 5519 K, which is very close to the old solution (see Fig 11, left). Also when using minmod (run rhd_minmod_hck) (see Fig 11 right) or the superbee reconstruction (run rhd_superbee_hck, now back with directional splitting, hdsplit = 123), we get normal temperature fluctuations. Minmod produces a very diffusive solution but the solution at $z = 1200$ km roughly agrees with the solutions obtained with PP and FRweno. Superbee produces a solution similar to PP but the problem with sawteeth and cold pixels is even worse. This job finally aborted because of a too small time step. However, granulation looks very good with Superbee: less diffusive than FRweno but smoother and almost as detailed as PP.

It seems that the problem with extreme temperature fluctuations near the top boundary occurs exclusively in the combination of VanLeer with hdsplit = 123. As of now, the reason for this behavior is unknown.

Summary and conclusions

The newly available reconstruction scheme, FRweno, remedies the problems that we experienced with PP in chromospheric layers. These problems do not disappear when using PP with the new code version. Generally, FRweno is more diffusive than PP but shows almost as much details as PP and is definitely less diffusive than VanLeer. When changing to higher spatial resolution (finer grids), all schemes reveal much more details in horizontal sections at all atmospheric heights, proving that the simulations are spatially not resolved. This is particularly true for the fligree

(bright intergranular filaments at locations of magnetic flux concentrations) which starts to look realistic for grid-cell sizes $\lesssim 10$ km only. Swirls tend to become less coherent at highest spatial resolution. The newly available option hdsplit = unsplit does not appreciably better than directional splitting but tends to be more fragile. There seems to be a problem with VanLeer in combination with directional splitting in that temperature fluctuations near the top boundary become large.

Freiburg. i. Br., 1. 7. 2013